Fluorescence Enhancement of Pyrene Chromophores Induced by Alkyl Groups through σ–π Conjugation: Systematic Synthesis of Primary, Secondary, and Tertiary Alkylated Pyrenes at the 1, 3, 6, and 8 Positions and Their Photophysical Properties

Yosuke Niko,[†] Susumu Kawauchi,[†] Shun Otsu,[†] Katsumi Tokumaru,[†] and Gen-ichi Konishi*,[†,‡]

[†]Department of Organic and Polymeric Materials, Tokyo Institute of Technology, O-okayama, Tokyo 152-8552, Japan
[‡]PRESTO, Japan Science and Technology Agency (JST), Kawaguchi, Saitama 332-0012, Japan

Ⓢ *Supporting Information*

ABSTRACT: We have systematically synthesized 1-, 3-, 6-, and 8-alkyl-substituted pyrene derivatives using the latest synthesis methods and investigated the effects of alkyl substitution on the photophysical properties of the pyrene chromophore. Like the trimethylsilyl group, which is known to enhance the fluorescence properties of some chromophores through σ^*–π^* conjugation, alkyl groups (primary, secondary, and tertiary) enhanced the fluorescence quantum yield of the pyrene chromophore through σ–π conjugation in most cases. While these enhancements in the fluorescence quantum yield were beyond expectations, the results were supported by absolute measurements. These results also indicate that ubiquitous alkyl groups can be used to tune the photophysical properties of the pyrene chromophore, as well as to improve the solubility or prevent aggregation. In other words, they can be used to develop new photofunctional materials.
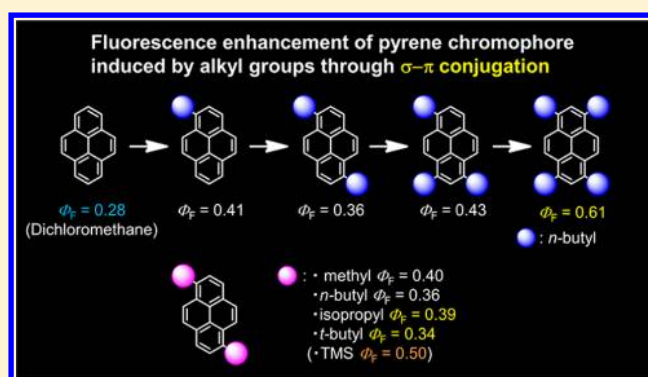
INTRODUCTION

Pyrene is a well-known chromophore and has been a typical candidate organic fluorescent material, e.g., as a probe in multimolecular systems[1−18] or as a metal ion sensor,[19−25] because of its environment-responsive vibrational fluorescence structures, long excited singlet lifetime, and ability to form excimers. In recent years, since pyrene and most of its derivatives have high absorption coefficients and fluorescence quantum yields, numerous investigations have been carried out on their use as highly emitting materials for organic electronic devices such as organic light-emitting diodes (OLEDs)[26−33] and liquid crystal lasers,[34,35] as well as solar cells.[36,37]

For these applications, the most general and important strategy for designing fluorescent materials based on the pyrene chromophore is to introduce substituents at the 1-, 3-, 6-, and 8-positions in the pyrene. For instance, it is widely known that the introduction of phenyl[38−46] and ethynyl groups[47−53] or trimethylsilyl (TMS)[48,54−60] and trimethylsilylmethyl (TMSM)[61] groups at the 1-, 3-, 6-, and 8-positions in pyrene expand the π-system and increase the oscillator strength,[39] resulting in dramatic improvements in the photoluminescence (PL) properties, especially in the fluorescence quantum yield. In addition, various functional groups such as carbonyl groups have been also used to modify the PL properties as well as the mechanisms of the PL in pyrene.[62−71] Furthermore, these pyrene dyes have often been introduced into sophisticated

structures such as spiro skeletons,[72] polymers,[73−78] cyclophanes,[79,80] calix arenes,[31,81] and inorganic matrixes[82,83] to obtain various desired functions.

However, the introduction of alkyl groups, which are the most ubiquitous substituents, to pyrene at the 1-, 3-, 6-, and 8-positions has not been performed in a systematic way. Therefore, how alkyl groups affect the PL properties of pyrene has not been discussed in detail, although alkylpyrene derivatives are often prepared and some have been studied individually.[61,84−92] Thus, in the field of organic material science in general, the introduction of alkyl groups was mostly carried out not to tune photophysical properties but to enhance the solubility and suppress π–π stacking.[61,93−95] In other words, it is often believed that alkyl groups do not significantly affect the PL properties of chromophores. On the other hand, it has been reported that in oligo-*p*-phenylene dyes and polycyclic aromatic hydrocarbon dyes such as naphthalene and anthracene, the introduction of a methyl group at an appropriate position sometimes changes the chromophore's properties such as its fluorescence quantum yield and lasing properties.[95] These effects can be due to the influence of hyperconjugation, steric hindrance, and/or changes in molecular symmetry. These reports suggest that understanding the
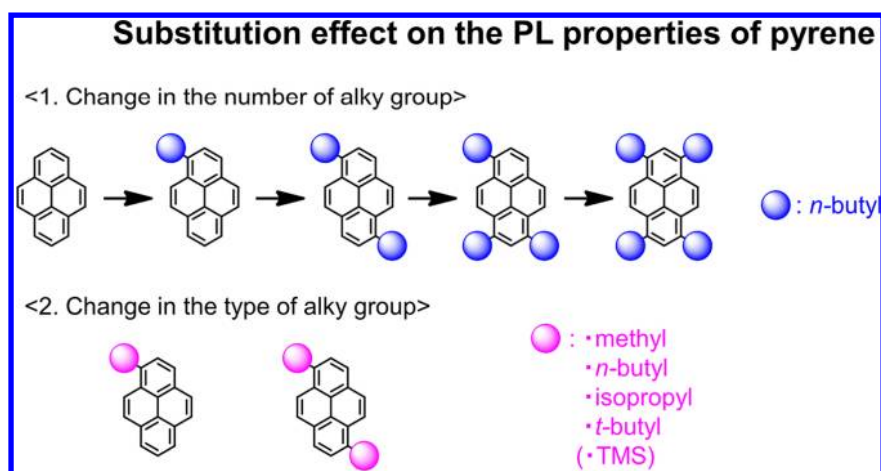
Figure 1. Main subject investigated in this work.

effect of alkyl substitutions on the photophysical properties of the pyrene chromophore is very valuable for versatile material design. In fact, recent developments in organic synthesis have enabled us to synthesize multiple pyrene derivatives with the 1-, 3-, 6-, and 8-positions modified symmetrically or asymmetrically with various substituents, including alkyl groups,[96−98] even though the introduction of bulky alkyl groups to pyrene at the 1-, 3-, 6-, and 8-positions had been difficult.[89,90]

To this end, we systematically synthesized mono-, di-, tri-, and tetra-alkylated pyrene derivatives containing butyl groups and, subsequently, investigated how the number of alkyl groups affects the photophysical properties of the pyrene chromophore (Figure 1). Next, pyrene derivatives functionalized by primary, secondary, and tertiary alkyl groups at the 1-position or at the 1- and 6-positions were prepared, and the differences in their photophysical properties due to the changes in the types of alkyl groups were examined. For comparison, the TMS group was also introduced to pyrene at the 1-position or at the 1- and 6-positions. While the TMS group does not possess a π-electron similar to that of an alkyl group, it is well-known that TMS groups affect the photophysical properties of chromophores through $\sigma^*-\pi^*$ conjugation.[99,100] Since the TMS group is known to be useful for the design of OLED and electron transport materials,[101−103] detailed comparisons between alkyl and TMS groups may result in expanded utility of the alkyl groups.

In this study, we used an absolute method for measuring the fluorescence quantum yield. Furthermore, molecular orbital calculations and an electrochemical method were also used to obtain mechanistic insight into the PL properties of pyrene derivatives. The absolute measurements revealed that in most cases all alkyl groups enhance the fluorescence quantum yield of pyrene, as does the TMS group. In addition, the calculations and electrochemical measurements showed that alkyl groups induced conjugation between C−H or C−C s orbitals and the p orbitals of pyrene and, as a result, the destabilization of the highest occupied molecular orbital (HOMO). The accompanying bathochromic shifts were observed in the UV−vis spectra, although the mechanism of these shifts is different from that when the TMS group was used. That is, the role of the alkyl groups in the tuning the photophysical properties of pyrene was more significant than expected. Therefore, it can be said that alkyl groups have significant but neglected effects on the photophysical properties of pyrene. These results indicate that alkyl groups serve to improve the PL properties of the pyrene

chromophore, as do other functional groups. Therefore, it can be expected that new photofunctional pyrene materials can be developed by strategically utilizing the substitution effects of alkyl groups and these other groups as well as by introducing such substituted chromophores into the sophisticated structures described above. We believe that the knowledge obtained in this paper will help in the development of new principles for more versatile material design based on pyrene with alkyl groups.

■ RESULTS AND DISCUSSION

Synthesis. As discussed in detail in a previous report,[54,55,84] **P1b** and **P1e** were synthesized as follows. 1-Bromopyrene was lithiated by *n*-BuLi and then treated with the corresponding electrophilic reagents, 1-bromobutane or chlorotrimethylsilane. Disubstituted derivatives **P2a**, **P2b**, and **P2e** were also obtained from 1,6-dibromopyrene in the same manner. Subsequently, after **P2b** was mono- or dibrominated,[96] **P3b** and **P4b** were prepared from the corresponding brominated pyrene derivatives (Scheme 1).

Both **P1c** and **P2c** were synthesized using the Negishi cross-coupling reaction.[104] **P1d** and **P2d** were prepared using the Kumada cross-coupling reaction,[105−107] which was recently improved by Joshi-Pangu et al.,[97] because the introduction of a tertiary butyl group into pyrene using the Friedel−Crafts reaction is mostly achieved at the 2- and 7-positions owing to steric hindrance.[89,90] In general, in Negishi or Kumada cross-coupling reactions where secondary or tertiary alkyl nucleophiles are used, isomers of the desired products are generated because of rapid β-hydride elimination. Similarly, in the syntheses of **P1c**, **P2c**, **P1d**, and **P2d**, the corresponding isomers were obtained, i.e., **P1c** and **P2c** substituted with an *n*-propyl group instead of an isopropyl group and **P1d** and **P2d** substituted with an isobutyl group instead of a *tert*-butyl group. The target compounds were isolated from their isomers by repeatedly performing high-performance liquid chromatography (HPLC) and recrystallization. Finally, the abundance ratios of the target compounds and their isomers were estimated by calculating the integral ratios of the corresponding alkyl groups in the ^{1}H NMR spectra: **P1c** (*i*-Pr:*n*-Bu) = 15:1, **P2c** (*i*-Pr:*n*-Bu) = 21:1, **P1d** (*t*-Bu:*i*-Bu) = 23:1, and **P2d** (*t*-Bu:*i*-Bu) = 62:1. Then, we decided to measure the photophysical and electrochemical properties of the compounds obtained without further purification, since the amounts of isomers that could not

Scheme 1. Synthetic Routes and Chemical Structures of Alkylpyrene Derivatives Used in This Work
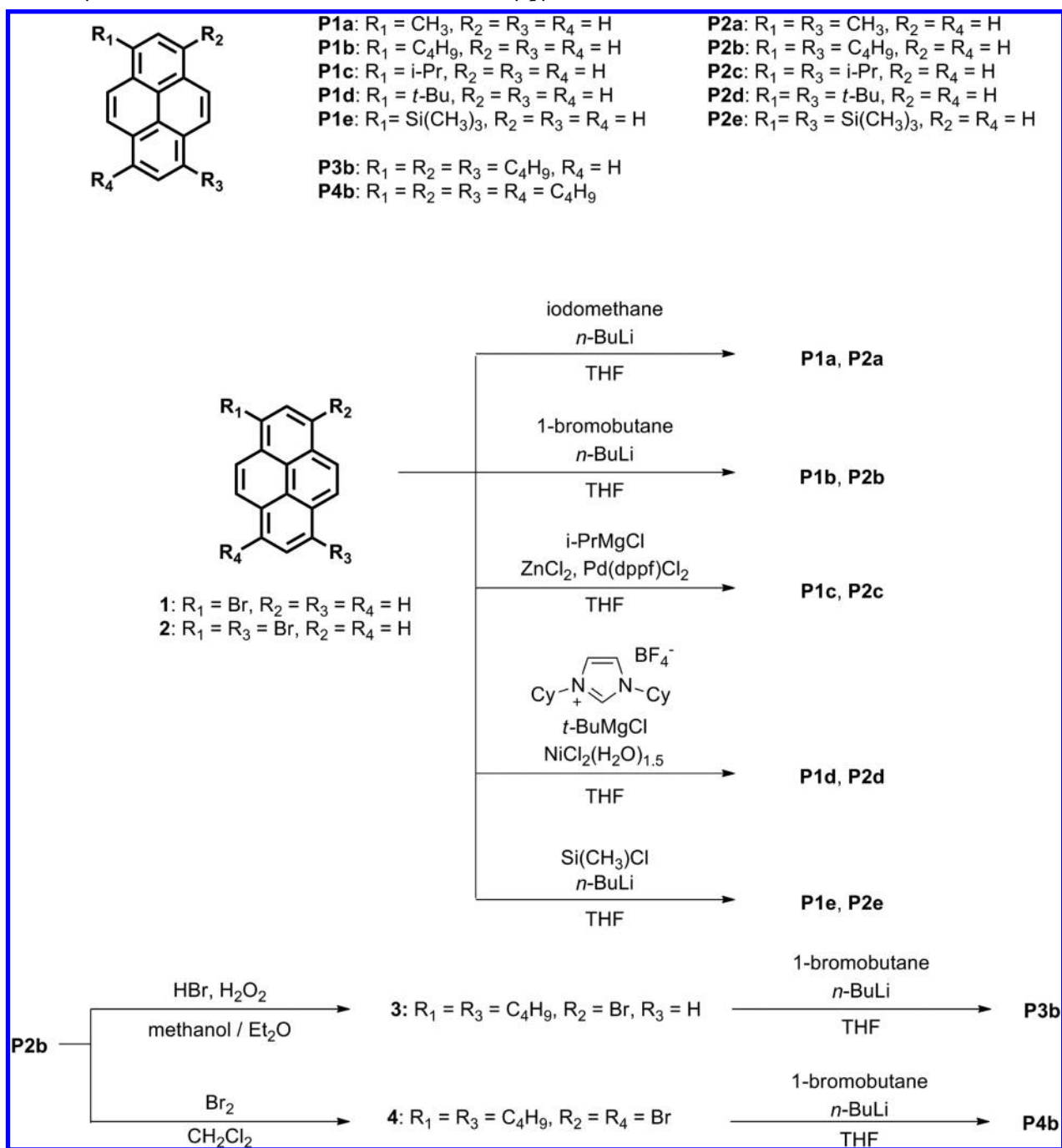
be removed appeared to be small enough to not significantly affect the results described below.

Effects of Number of Alkyl Groups on the Photophysical Properties of Pyrene: Comparison between Parent Pyrene P0 and P1b−P4b. First, the UV−vis and PL spectra, absolute fluorescence quantum yields, and fluorescence lifetime decay of **P0** and **P1b−P4b** were measured in deaerated hexane, dichloromethane, and methanol in order to understand the effect of the number of alkyl substituents on the photophysical properties of pyrene. Next, to study the changes in the frontier orbitals, the HOMO and the lowest unoccupied molecular orbital (LUMO) levels were estimated by measuring the oxidation potentials obtained using square wave voltammetry. Furthermore, to examine the PL processes of the pyrene

derivatives in detail, their optimized structures in the ground state under vacuum conditions were calculated using the density functional theory (DFT) method at the ωB97X-D/6-31G(d,p) level,[108−112] which is suited to deal with the excited states because this method includes both long-range correction and dispersion correction.[113,114] Subsequently, the oscillator strengths and the singlet and triplet energies were obtained by performing time-dependent DFT (TD-DFT) calculations.

Measurement of UV−vis and PL Spectra, Absolute Fluorescence Quantum Yields, and Fluorescence Lifetime Decay. As described in Figure 2, upon the introduction of butyl groups, the UV−vis spectra of **P0** and **P1b−P4b** showed a stepwise bathochromic shift. The maximum absorption wavelength, $\lambda_{abs,max}$, was shifted about 6−8 nm per butyl group
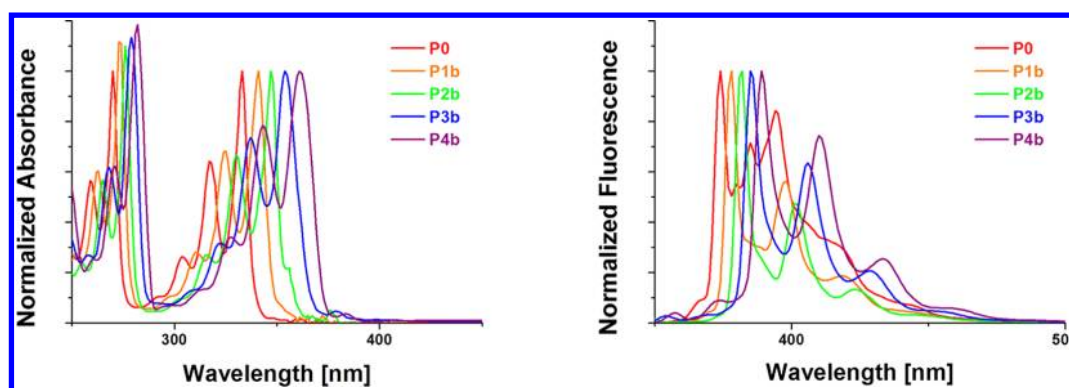
Figure 2. UV−vis and fluorescence spectra of **P0** and **P1b**−**P4b** (DCM, rt, $\lambda_{ex} = \lambda_{abs,max}$).

Table 1. Spectroscopic Parameters of P0 and P1b−P4b

entry	solvent	log ε	$\lambda_{abs,max}$ [nm]	$\lambda_{em,max}$ [nm]	τ [ns]	Φ_F	k_f^{*a} [10^7 s^{-1}]	k_{nr}^{b} [10^9 s^{-1}]
P0	Hex	4.62	330	373	78.9	0.23	0.29	0.98
	DCM		333	374	104.4	0.28	0.27	0.69
	MeOH		330	373	110.0	0.17	0.15	0.75
P1b	Hex	4.66	338	377	69.1	0.35	0.51	0.94
	DCM		341	378	63.0	0.41	0.65	0.94
	MeOH		338	377	152.4	0.31	0.20	0.45
P2b	Hex	4.65	344	380	57.8	0.47	0.81	0.92
	DCM		347	382	42.0	0.36	0.86	1.52
	MeOH		344	381	70.6	0.60	0.85	0.57
P3b	Hex	4.65	352	384	59.0	0.49	0.83	0.86
	DCM		354	385	49.4	0.43	0.87	1.15
	MeOH		351	384	78.1	0.60	0.77	0.51
P4b	Hex	4.69	359	388	65.8	0.55	0.84	0.68
	DCM		361	389	56.7	0.61	1.08	0.69
	MeOH		358	388	75.0	0.67	0.89	0.44

$^a k_f = \Phi_F / \tau$. $^b k_{nr} = (1 - \Phi_F) / \tau$.

(Table 1). This implies that the HOMO-LUMO band gaps of **P0** and the alkylated pyrenes (ΔE(HOMO-LUMO)) tend to become narrower with increases in the number of butyl groups. Such redshifts were also seen for the (0−0) band in the PL spectra of **P0** and **P1b**−**P4b**. While the highly structured fluorescence of **P0**, which is widely known as the Ham effect,[115] was not retained after monosubstitution, **P1b**−**P4b** also showed clear vibrational structures in the UV−vis and PL spectra.

As seen in Table 1, **P1b**−**P4b** showed higher fluorescence quantum yields (Φ_F) compared with that of **P0**. In addition, except for the case of **P1b** and **P2b** in dichloromethane, the Φ_F values increased gradually with increasing number of butyl groups. In particular, in fully substituted **P4b**, very high Φ_F values were observed: 0.55, 0.61, and 0.67 in hexane, dichloromethane, and methanol, respectively. Because the weak fluorescence of the parent pyrene is derived from the forbidden $S_1 \rightarrow S_0$ (often called $^1L_b \rightarrow ^1A$) transition, it can be deduced that such enhanced fluorescence of **P1b**−**P4b** might be derived from the allowed $S_1 \rightarrow S_0$ (often called $^1L_a \rightarrow ^1A$) transition, as is the case for 1,3,6,8-tetraphenylpyrene.[39] In any case, as described below, these values were much higher than expected, which indicates that alkyl groups might be useful for tuning the photophysical properties of pyrene derivatives.

Square Wave Voltammetry. Square wave voltammetry measurements in oxygen-free dichloromethane solution were carried out to examine the electrochemical properties of **P0** and **P1b**−**P4b**. As is evident from Figure S6 in Supporting Information, the oxidation potentials E^{OX}, which are the values for the first peak top, shifted toward the negative side in a stepwise manner upon the introduction of butyl groups. Here, the HOMO and LUMO levels were estimated by combining the UV−vis spectral data and electrochemical data; the values are listed in Table 2.

Table 2. Electrochemical Properties of P0 and P1b−P4b

entry	$E_{ox}{}^a$ [V]	HOMO^b [eV]	$\lambda_{onset}{}^c$ [nm]	LUMO^d [eV]	ΔE(LUMO-HOMO) [eV]
P0	1.12	−5.68	341	−2.05	3.64
P1b	1.03	−5.60	349	−2.04	3.55
P2b	0.93	−5.49	359	−2.04	3.45
P3b	0.83	−5.40	367	−2.02	3.38
P4b	0.74	−5.31	373	−1.98	3.32

$^a E^{OX}$ is the value of the first peak top in square wave voltammetry analysis. ^{b}The HOMO was determined from the oxidation potential using the relationship HOMO = $-e[E^{OX} - 0.234] - 4.8$ eV, where +0.234 V is the redox potential for the ferrocene/ferrocenium (Fc/Fc$^+$) couple, measured as an external standard for the system, versus a nonaqueous Ag/Ag$^+$ reference electrode; -e is a notation indicating the acceleration of one electron through the adjusted potential; and −4.8 eV represents the work function of the Fc/Fc$^+$ couple relative to the vacuum level.[116] $^c\lambda_{onset}$ are taken as the intersection of spectrum baseline and a tangent line to edge of the absorption band.[116] ^{d}LUMO was deduced from the optical band gap using the expression LUMO = HOMO + λ_{onset}.
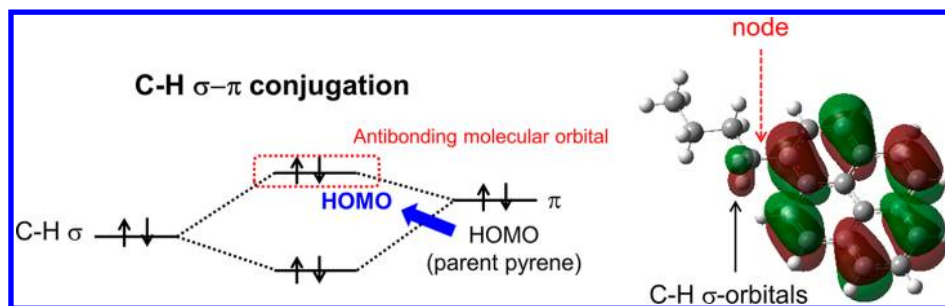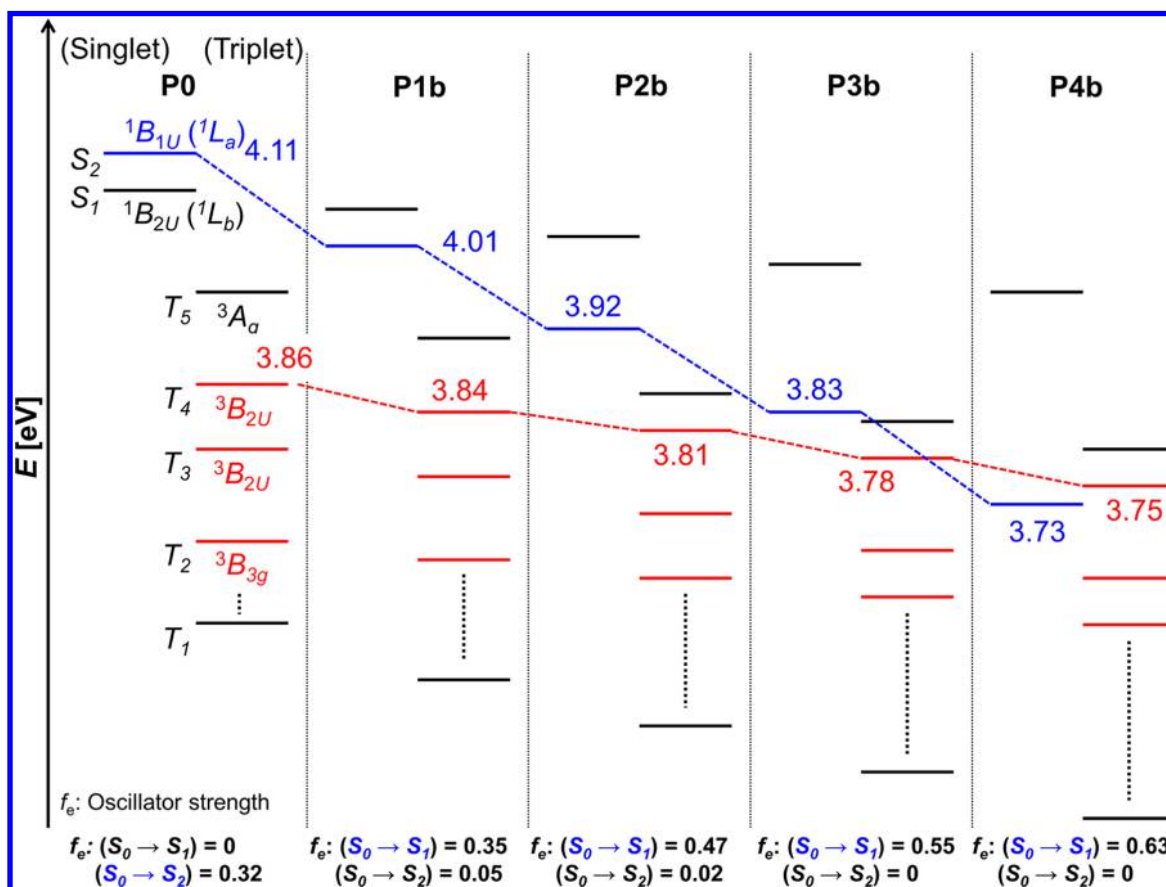
Figure 3. Frontier orbital interaction diagram of **P1b**.

Figure 4. Singlet and triplet states and oscillator strengths of **P0** and **P1b–P4b** simulated by TD-DFT (ωB97X-D/6-31G(d,p)).

In these investigations, it was found that the HOMO and LUMO levels were destabilized by about 0.08–0.11 and 0–0.04 eV per butyl group, respectively. While this trend is common when a donor molecule is introduced into a π-system, this is the first clear and systematic demonstration for alkylated pyrene derivatives.

DFT/TD-DFT Calculations. The results of the DFT/TD-DFT calculations agreed well with the experimental results. Here, we note the following three important trends for interpreting the fluorescence behaviors of **P0** and **P1b–P4b**.

(1) Frontier orbital interaction between the C–H σ-orbital of the alkyl groups and the π-orbitals of pyrene was observed (Figure 3).

The HOMO of **P1b** described by the DFT calculation indicates that the butyl groups interact with the pyrene unit. In addition, this interaction was also observed in MOs of **P2b–P4b** (see Figure S13 in Supporting Information). Because the MOs are antibonding, it can be understood that $\sigma-\pi$

conjugation, i.e., hyperconjugation, occurred. Furthermore, because of the $\sigma-\pi$ conjugation, the HOMOs of **P1b–P4b** were destabilized in a stepwise manner (see Figure S9 in Supporting Information). On the other hand, the LUMOs were destabilized to a smaller extent relative to the HOMOs. As a result, the HOMO-LUMO band gaps became narrower after the introduction of butyl groups. Such a reduction in the HOMO-LUMO band gaps agreed well with the bathochromic shifts observed in the UV–vis spectra. In addition, the behaviors of the HOMO and LUMO levels were similar to those observed in the square wave voltammetry analysis. Thus, the bathochromic shifts observed upon the introduction of butyl groups into the pyrene chromophore likely resulted from $\sigma-\pi$ conjugation between the butyl groups and pyrene.

(2) The oscillator strengths (f_e) of pyrene derivatives at the HOMO→LUMO transition, i.e., $^1A\rightarrow^1L_a$, were gradually increased upon the introduction of butyl groups (Figure 4).
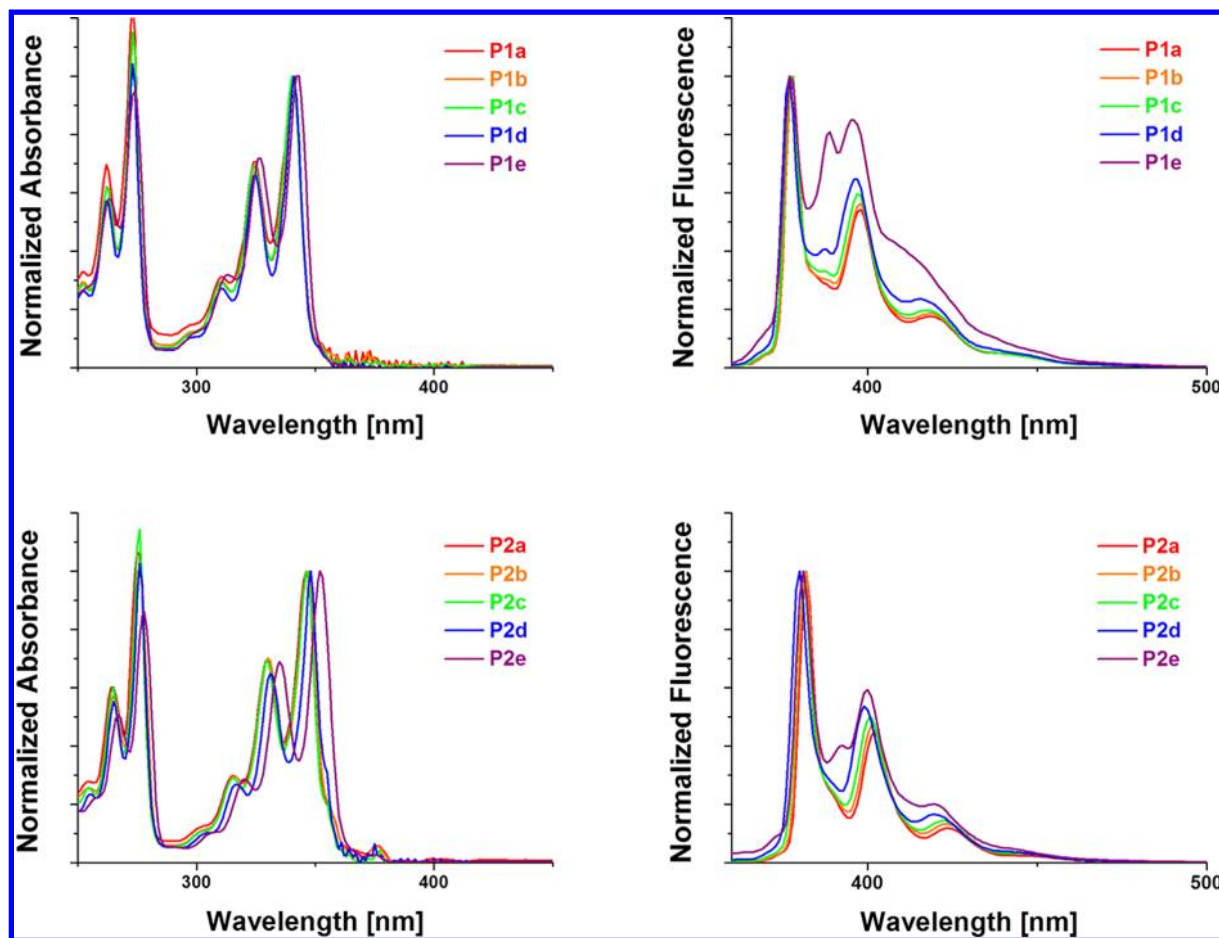
Figure 5. UV−vis and fluorescence spectra of (top) **P1a−e** and (bottom) **P2a−e** (DCM, rt, $\lambda_{ex} = \lambda_{abs,max}$).

In general, a proportional relationship exists between the oscillator strength and the absorption coefficient (ε). However, such a relationship was not clear from the experimentally obtained ε values of **P0** and **P1b−P4b**, probably because the changes were too small relative to the experimental errors (Table 1). On the other hand, the radiative rate constants (k_f) increased with increasing number of butyl groups under almost all conditions. Because k_f is often correlated with the oscillator strength,[95] trend 2 can be considered to correspond with the experimental results. Furthermore, it can be said that such an increase in k_f is one of the reasons for the enhancement of Φ_F after the introduction of butyl groups.

(3) The excited singlet states derived from the HOMO→LUMO transitions (second singlet excited state S_2 for **P0** and first singlet excited state S_1 for **P1b−P4b**) were greatly stabilized relative to the adjacent triplet states ($T_2−T_5$), and as a result, the energy gaps between the S_1 states and adjacent triplet states became narrower or the potential levels between S_1 and the adjacent triplet states were inverted (Figure 4).

This is a very important trend related to the PL properties of pyrene derivatives. First, as mentioned above, while the fluorescence of parent pyrene is derived from forbidden $S_1 \rightarrow S_0$ transition, the potentials of the S_1 and S_2 states of the parent pyrene were inverted after the introduction of butyl groups. Thus, the fluorescence of **P1b−P4b** was derived from allowed transitions. This change is also a factor driving the enhancement of Φ_F. Next, intersystem crossing, one of the fluorescence deactivation processes, depends on the energy gap between S_1 and adjacent triplet states according to energy gap law.[115]

Usually, for polycyclic aromatic hydrocarbon dyes in deaerated condition, Φ_F is expressed as $\Phi_F = k_f/(k_f + k_{nr})$, $k_{nr} = k_{IC} + k_{ISC} + k[O_2] = k_{ISC}$, where k_f, k_{nr}, k_{IC}, k_{ISC}, and $k[O_2]$ represent the rate constants for fluorescence radiation, nonradiative decay, internal conversion, intersystem crossing, and quenching by dioxygen, respectively.[115] Therefore, Φ_F is dependent on k_{ISC}, i.e., the energy gap between S_1 and its adjacent triplet states. As an example, the introduction of alkyl groups into a chromophore changes Φ_F dramatically, as in the well-known relationship between anthracene ($\Phi_F = 0.24$) and 9,10-dimethylanthracene ($\Phi_F = 0.68$).[95] This phenomenon is explained as follows. According to first-order perturbation theory, in anthracene, efficient intersystem crossing occurs between $S_1(^1B_{1U})$ and the adjacent $T_n(^3B_{2U})$. Introduction of methyl groups at the 9,10-positions inverts the potential level between $S_1(^1B_{1U})$ and $T_n(^3B_{2U})$, which suppresses the deactivation process and enhances Φ_F. Here, we observe a similar phenomenon for pyrene and its alkylated derivatives. In other words, the change in Φ_F upon the introduction of butyl groups into pyrene is derived from the difference in the energy gap between the $S_1(^1B_{1U})$ and $T_n(^3B_{2U})$ states of pyrene. This hypothesis can also be used to interpret some of the commonly observed PL characteristics of pyrene derivatives, such as the decrease in Φ_F upon the introduction of butyl groups and the changes in Φ_F caused by solvent changes. In particular, when the energy potentials of the $S_1(^1B_{1U})$ and $T_n(^3B_{2U})$ states of pyrene become close to each other because of the introduction of butyl groups or because of solvent changes, Φ_F is reduced. On the other hand, when the energy levels of $S_1(^1B_{1U})$ and

Table 3. Spectroscopic Parameters of P1a–e and P2a–e

entry	solvent	log ε	λ_{abs} [nm]	λ_{em} [nm]	τ [ns]	Φ_F	k_f [10^7 s^{-1}]	k_{nr} [10^9 s^{-1}]
P1a	Hex	4.66	338	377	67.8	0.34	0.50	0.97
	DCM		341	378	79.1	0.45	0.57	0.70
	MeOH		338	377	132.0	0.28	0.21	0.55
P1b	Hex	4.66	338	377	76.8	0.37	0.48	0.82
	DCM		341	378	63.0	0.41	0.65	0.94
	MeOH		338	377	152.4	0.31	0.20	0.45
P1c	Hex	4.65	338	376	50.6	0.21	0.42	1.56
	DCM		340	377	77.8	0.41	0.53	0.76
	MeOH		337	376	149.2	0.24	0.16	0.51
P1d	Hex	4.66	338	376	67.4	0.26	0.39	1.10
	DCM		341	377	86.0	0.38	0.44	0.72
	MeOH		338	376	154.8	0.21	0.14	0.51
P1e	Hex	4.66	340	346	66.9	0.23	0.34	1.15
	DCM		343	377	94.2	0.36	0.38	0.68
	MeOH		340	376	174.6	0.22	0.13	0.45
P2a	Hex	4.64	344	380	54.7	0.52	0.95	0.88
	DCM		346	382	37.6	0.40	1.06	1.60
	MeOH		344	381	64.5	0.56	0.87	0.68
P2b	Hex	4.65	344	380	57.8	0.47	0.81	0.92
	DCM		347	382	42.0	0.36	0.86	1.52
	MeOH		344	381	70.6	0.60	0.85	0.57
P2c	Hex	4.65	345	380	52.9	0.45	0.85	1.04
	DCM		346	381	40.3	0.39	0.97	1.51
	MeOH		343	380	85.7	0.55	0.64	0.53
P2d	Hex	4.70	346	379	60.9	0.43	0.71	0.94
	DCM		348	380	43.1	0.34	0.79	1.53
	MeOH		345	379	78.6	0.54	0.69	0.59
P2e	Hex	4.72	350	380	53.7	0.42	0.78	1.08
	DCM		352	381	65.5	0.50	0.76	0.76
	MeOH		349	380	71.8	0.50	0.70	0.70

$T_n(^3B_{2U})$ are inverted or are very different from each other, Φ_F is enhanced. From these trends, it can be concluded that **P4b** showed the largest k_f and the smallest k_{nr} under all conditions, because trends (2) and (3) suggest that the oscillator strength increased with a concurrent inversion of the energy potentials between $S_1(^1B_{1U})$ and $T_n(^3B_{2U})$ upon the introduction of four butyl groups.

To summarize, butyl groups attached to the 1-, 3-, 6-, and 8-positions of the pyrene chromophore give rise to an important effect: $\sigma-\pi$ conjugation. Both bathochromic shifts in the UV–vis spectra reflecting destabilization of the HOMO and the increase in k_f upon the introduction of butyl groups are caused by $\sigma-\pi$ conjugation. Moreover, the expansion of the π-system due to the butyl groups at the 1-, 3-, 6-, and 8-positions tends to change the fluorescence mechanism from a forbidden to an allowed transition and to suppress intersystem crossing, because the S_1 energy potentials are greatly stabilized relative to the adjacent triplet states. As a result, the fluorescence quantum yield is strongly enhanced. On the other hand, the simple introduction of a butyl group does not always enhance the Φ_F of pyrene, as evidenced by the smaller Φ_F of **P2b** compared to that of **P1b** in dichloromethane.

Differences Caused by the Change in the Type of Alkyl Group: Comparison of Photophysical Properties of Primary, Secondary, and Tertiary Alkyl-Substituted Pyrenes at 1- and 1,6-Positions (P1a–P1d and P2a–P2d). To understand the changes in the PL properties caused by the different alkyl groups, **P1a**, **P1c**, and **P1d** substituted with primary, secondary, and tertiary alkyl groups, respectively

(Scheme 1), and their disubstituted derivatives, i.e., **P2a**, **P2c**, and **P2d**, were investigated in the same manner as **P1b–P4b**.

As can be seen in Figure 5 and Table 3, the UV–vis and PL spectra of the alkylated pyrenes showed very small changes in their vibrational structures and wavelengths for the different alkyl groups. Square wave voltammetry measurements also revealed that the HOMO and LUMO levels of **P1a–d** and **P2a–d** were almost identical (Table 4, Figures S7 and S8 in Supporting Information). The results of the MO calculations, which were performed in the same manner as those for **P0** and **P1b–P4b**, agreed with these results (see Figure S10 in Supporting Information). It should be noted here that not only the C–H σ-orbital but also the C–C σ-orbitals of secondary and tertiary alkylated pyrene derivatives participated

Table 4. Electrochemical Properties of P1a–e and P2a–e

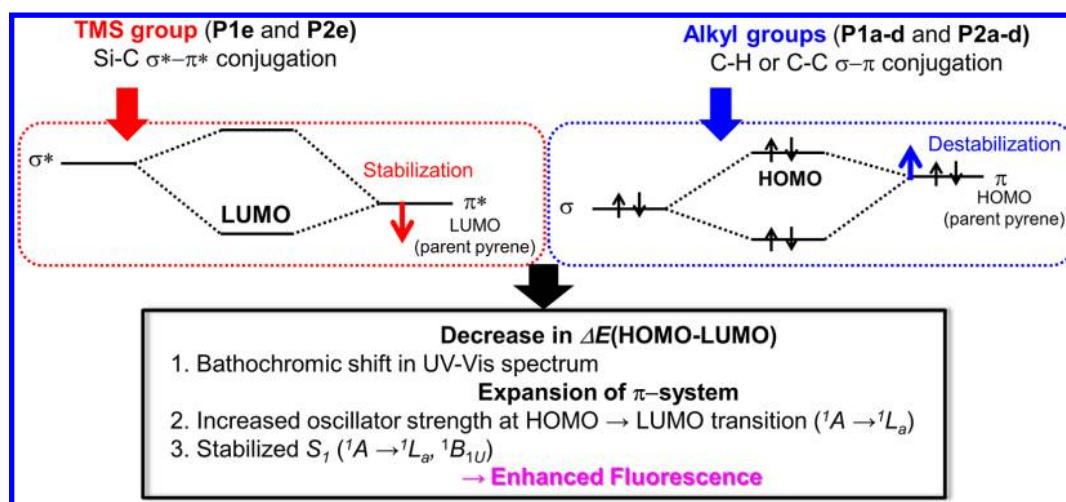| entry	E_{ox} [V]	HOMO [eV]	λ_{onset} [nm]	LUMO [eV]	E(LUMO-HOMO) [eV]
P1a	1.02	−5.59	349	−2.04	3.55
P1b	1.03	−5.60	349	−2.04	3.55
P1c	1.02	−5.59	349	−2.03	3.55
P1d	1.03	−5.60	349	−2.04	3.55
P1e	1.06	−5.62	351	−2.09	3.53
P2a	0.93	−5.49	360	−2.05	3.44
P2b	0.93	−5.49	359	−2.04	3.45
P2c	0.93	−5.49	359	−2.04	3.45
P2d	0.94	−5.51	360	−2.07	3.43
P2e	1.03	−5.59	363	−2.18	3.42

Figure 6. Comparison of the effects of substitution of alkyl and TMS groups.

in the $\sigma-\pi$ conjugation in the HOMOs (see Figure S13 in Supporting Information). Next, while no notable changes were observed in the fluorescence quantum yields, as a possible trend, the Φ_F values of the secondary and tertiary alkylated pyrenes were slightly smaller than those of the primary alkylated ones. This difference in Φ_F might result from the loose bolt effect,[115] which is seen in the relationship between toluene and *tert*-butylbenzene. In particular, the fluorescence deactivation processes caused by internal conversion in the secondary or tertiary alkylated pyrene derivatives were more effective than those in the primary alkylated ones. In addition, the differences in the fluorescence quantum yields, absorption/fluorescence wavelengths, and HOMO/LUMO levels between **P1a−d** and **P2a−d** were almost the same as those between **P1b** and **P2b** (Tables 1 and 3).

Thus, these results show that substitution with primary, secondary, and tertiary alkyl groups causes no significant change in the photophysical properties. In other words, both secondary and tertiary alkyl groups serve to enhance the fluorescence quantum yield of pyrene by participating in the $\sigma-\pi$ conjugation, in a similar way to the primary alkylated pyrenes. In the context of recent efforts devoted to the development of dyes that show strong emission even in the aggregated state,[27,117−120] this knowledge is very important for the molecular design of PL materials, since the introduction of bulky substitutes is the most popular methodology for preventing $\pi-\pi$ stacking or improving solution processability. In fact, in contrast to the parent pyrene, **P2d** did not show excimer emission under concentrated conditions, which demonstrates that the tertiary butyl group certainly served to prevent the aggregation between pyrene chromophores (see Figures S4 and S5 in Supporting Information). Moreover, very recently it was demonstrated that the introduction of a bulky isopropyl group at the 1-, 3-, 6-, and 8-positions of pyrene suppressed excimer formation.[91]

Differences Caused by the Change in $\sigma-\pi$ Conjugation: Comparison of Photophysical Properties between Trimethylsilyl-Substituted Pyrenes and 1- and 1,6-Alkylpyrenes. Finally, we reinvestigated the photophysical properties of **P1e** and **P2e** as typical compounds with $\sigma-\pi$ conjugation in order to understand the difference between the $\sigma-\pi$ conjugation caused by C−H or C−C σ-orbitals and the conjugation caused by Si−C σ-orbitals.[48,55−57] For this

purpose, we compared **P1e** and **P2e** with other alkylated pyrene derivatives.

As described in Figure 5, **P1e** and **P2e** showed larger bathochromic shifts than did **P1a−d** and **P2a−d**, respectively. Furthermore, as mentioned by Matsumoto and Yamaguchi et al.,[99,100] square wave voltammetry analysis indicates that such bathochromic shifts are caused by the greater stabilization of the LUMO as compared to the HOMO (see Figures S7 and S8 in Supporting Information). In other words, while both the TMS group and the alkyl group can cause bathochromic shifts of the UV−vis spectra in pyrene, the corresponding mechanisms underlying the reduction in the HOMO-LUMO band gap are sharply different. The calculated MOs of **P1e** and **P2e** also suggest that the stabilization of both the HOMO and LUMO resulted from $\sigma*-\pi*$ conjugation between the $\sigma*$-orbitals of the weak Si−C bond and the $\pi*$-orbitals of pyrene and that the contributions of this $\sigma*-\pi*$ conjugation to the LUMO levels are much larger than the contributions to the HOMO levels (see Figures S10 and S13 in Supporting Information).

Interesting results were obtained from the measurements of the fluorescence quantum yields. The PL properties of dyes that show $\sigma*-\pi*$ conjugation between various Si−C σ-orbitals and chromophores has been investigated previously. It has been reported that Si−C substituents such as trimethylsilyl and trimethylsilylmethyl can improve the fluorescence quantum yields of the chromophores.[48,55−59,61,99] However, in our results, the enhancement of Φ_F upon the introduction of a TMS group was not much different from that caused by the introduction of an alkyl group. Moreover, since the Φ_F of tetrakis(trimethylsilyl)pyrene is 0.57 in cyclohexane,[57] it can be said that the tetraalkylated **P4b** also fluoresces strongly.

To summarize, the main differences between the effect of TMS and the effect of the alkyl groups on the photophysical properties of pyrene are how they change the HOMO-LUMO band gap and the degrees of those changes. Both TMS and the alkyl groups enhance the Φ_F of the pyrene chromophore to the same extent (Figure 6). These results provide additional insights into the previously reported photophysical properties of pyrene.[55,56]

Importance of the Measurement of Absolute Fluorescence Quantum Yield. We also want to comment on the significance of the absolute fluorescence quantum yield of dyes in this mechanistic discussion of PL properties. Hardly any

research has been carried out in which the changes in the PL properties, especially those in the fluorescence quantum yields, caused by Si−C $\sigma^*-\pi^*$ and C−H or C−C $\sigma-\pi$ conjugations are compared. Furthermore, in-depth evaluation of the fluorescence quantum yields could not be performed for Si−C and C−H or C−C functionalized chromophores, especially for pyrene, because of the lack of measurements based on absolute methods and with uniform measurement conditions. However, very recently, it is easier to measure the absolute fluorescence quantum yield by using the integral sphere than before, due to the development of the studies as organic electronics devices such as OLEDs. In this study, while we demonstrated that alkyl groups can enhance the PL properties of the pyrene chromophore, as does the trimethylsilyl group, these notable and unexpected results were mainly supported by absolute fluorescence quantum yield measurements obtained under uniform measurement conditions including argon bubbling time. Thus, it is the absolute fluorescence quantum yield measurements that may change the common opinion regarding ubiquitous substitutions such as alkyl groups and their effect on the PL properties.

CONCLUSIONS

We synthesized alkylpyrene derivatives—mono-, di-, tri-, and tetra-butyl pyrenes with substitution at the 1-, 3-, 6-, and 8-positions (**P1b**–**P4b**) and primary, secondary, and tertiary alkyl-substituted pyrenes at the 1- or 1- and 6-positions (**P1a**–**P1d** and **P2a**–**P2d**)—systematically using the latest synthesis methods. In addition, the TMS group, which does not possess π electrons, was also introduced into the pyrene chromophore at the 1- or 1- and 6-positions (**P1e** and **P2e**). First, it was found that UV−vis and PL spectra of **P1b**–**P4b** were red-shifted with increases in the number of butyl groups. Moreover, the butyl groups enhanced the fluorescence quantum yields of the pyrene chromophore to a much greater extent than expected. Square wave voltammetry and DFT/TD-DFT calculations demonstrated that these substitution effects were mainly caused by $\sigma-\pi$ conjugation between the butyl groups and pyrene, which destabilized the HOMO of pyrene.

Next, no significant differences due to changes in the type of alkyl group were observed in the properties of **P1a**–**P1d** and **P2a**–**P2d**. It should be noted that both C−H and C−C σ bonds participated in the $\sigma-\pi$ conjugation. Finally, in the comparison of **P1e** and **P2e** with the alkylpyrene derivatives, it was demonstrated that both TMS and alkyl groups caused bathochromic shifts of the UV−vis spectra and enhanced the Φ_F value of the pyrene chromophore. Contrary to our expectations, the degree of enhancement in the Φ_F of **P1e** and **P2e** was the same as that in the corresponding alkylpyrene derivatives. On the other hand, the bathochromic shifts caused by the TMS group were derived from $\sigma^*-\pi^*$ conjugations, which were different from the $\sigma-\pi$ conjugations in the alkylpyrene derivatives. Thus, these results indicate that ubiquitous alkyl groups serve not only to improve the solubility and suppress the aggregation of dyes but also to enhance the PL properties, although alkyl groups do not always work in this manner. Because pyrene has these advantages of versatility in molecular design, including the introduction to multimolecular systems and other sophisticated structures such as cyclophane and calix arene, the above-mentioned information is expected to contribute to the development of new photofunctional materials. In the future, we plan to focus on the development of unique fluorescent materials using the effects of alkyl groups as

the key factors. In addition, we will also investigate the effects of alkyl group substitution on the PL properties of other polyaromatic hydrocarbons such as perylene and conjugated polymers.

EXPERIMENTAL SECTION

General Procedure A: Compounds Obtained from Mono-lithiated Pyrene (P1b, P3b, and P1e). To a solution of 1-bromopyrene derivative **1** or **3** (1.0 equiv) in tetrahydrofuran (THF) was added a 2.6 M solution of *n*-butyllithium in hexane (1.5 equiv) dropwise under an argon atmosphere at −78 °C. The reaction mixture was stirred at this temperature for 30 min, and then the corresponding electrophilic agent (1.5 equiv; **P1b** and **P3b**: 1-bromobutane; **P1e**: trimethylsilyl chloride) was added dropwise to the solution. The mixture was allowed to gradually warm to room temperature and then stirred for 3 h. After quenching the reaction with water, the organic layer was extracted with diethyl ether and dried over MgSO₄. The solvent was removed in vacuo, and the residue was purified by short-plug column chromatography on silica gel (hexane), high-performance liquid chromatography, and subsequent recrystallization in ethanol to give the target compounds.

Synthesis of 1-Butylpyrene (P1b). **P1b** was synthesized according to Procedure A. Colorless solid; yield 75% (0.38 g); mp 62.1−64.0 °C; ¹H NMR (400 MHz, CDCl₃, ppm) δ 8.29 (d, *J* = 9.3 Hz, 1H), 8.17−7.95 (m, 7H), 7.87 (d, *J* = 7.8 Hz, 1H), 3.35 (t, *J* = 7.8 Hz, 2H), 1.85 (tt, *J* = 7.6 Hz, 7.8 Hz, 2H), 1.52 (tq, *J* = 7.3 Hz, 7.6 Hz, 2H), 1.00 (t, *J* = 7.3 Hz, 3H); ¹³C NMR (100 MHz, CDCl₃, ppm) δ 137.3, 131.4, 130.9, 129.7, 128.6, 127.5, 127.2, 127.0, 126.4, 125.7, 125.1, 125.0, 124.7, 124.6, 123.5, 34.1, 33.3, 22.9, 14.1; MS (DART) calcd for C₂₀H₁₉ 259.1, found 259.1 ([M + H]⁺). Anal. Calcd for C₂₀H₁₈: C, 92.67; H, 7.02. Found: C, 92.67; H, 6.66.

Synthesis of 1-(Trimethylsilyl)pyrene (P1e). **P1e** was synthesized according to Procedure A. Colorless solid; yield 74% (0.36 g); mp 109.1−111.0 °C; ¹H NMR (400 MHz, CDCl₃, ppm) δ 8.47 (d, *J* = 9.2 Hz, 1H), 8.29−8.03 (m, 8H), 0.70 (s, 9H); ¹³C NMR (100 MHz, CDCl₃, ppm) δ 135.2, 131.7, 131.6, 130.9, 130.2 127.4, 127.3, 127.1, 126.7, 125.4, 124.7, 124.6, 124.5, 124.2, 123.7, 0.3; MS (DART) calcd for C₁₉H₁₈Si 274.1178, found 274.1195 ([M]⁺).

General Procedure B: Compounds Obtained from Dilithi-ated Pyrene (P2a, P2b, P4b, and P2e). To a solution of 1,6-dibromopyrene **2** or its derivative **4** (1.0 equiv) in THF was added dropwise a 2.6 M solution of *n*-butyllithium in hexane (6.0 equiv) under an argon atmosphere at 0 °C. The reaction mixture was stirred at this temperature for 12 h, and then the corresponding electrophilic agent (6.0 eq; **P2a**: iodomethane; **P2b** and **P4b**: 1-bromobutane; **P2e**: trimethylsilyl chloride) was added dropwise to the solution. The mixture was allowed to gradually warm to room temperature and then stirred for 3 h. After quenching the reaction with water, the organic layer was extracted with diethyl ether and dried over MgSO₄. The solvent was removed in vacuo, and the residue was purified by short-plug column chromatography on silica gel (hexane), high-performance liquid chromatography, and subsequent recrystallization in ethanol to give the target compounds.

Synthesis of 1,6-Dimethylpyrene (P2a). **P2a** was synthesized according to Procedure B. Pale yellow solid; yield 82% (1.36 g); mp 167.6−169.4 °C; ¹H NMR (400 MHz, CDCl₃, ppm) δ 8.17 (d, *J* = 9.2 Hz, 2H), 8.07 (d, *J* = 7.7 Hz, 2H), 8.06 (d, *J* = 9.2 Hz, 2H), 7.85 (d, *J* = 7.7 Hz, 2H), 2.97 (s, 3H); ¹³C NMR (100 MHz, CDCl₃, ppm) δ 131.9, 129.5, 129.4, 127.8, 127.2, 124.9, 124.4, 122.6, 19.9; MS (DART) calcd for C₁₈H₁₄ 230.1096, found 230.1091 ([M]⁺).

Synthesis of 1,6-Dibutylpyrene (P2b). **P2b** was synthesized according to Procedure B. Pale yellow solid; yield 78% (2.05 g); mp 97.6−98.8 °C; ¹H NMR (400 MHz, CDCl₃, ppm) δ 8.21 (d, *J* = 9.2 Hz, 2H), 8.07 (d, *J* = 7.7 Hz, 2H), 8.04 (d, *J* = 9.2 Hz, 2H), 7.84 (d, *J* = 7.7 Hz, 1H), 3.32 (t, *J* = 7.8 Hz, 2H), 1.83 (tt, *J* = 7.4 Hz, 7.8 Hz, 4H), 1.51 (tq, *J* = 7.3 Hz, 7.4 Hz, 4H), 0.99 (t, *J* = 7.3 Hz, 6H); ¹³C NMR (100 MHz, CDCl₃, ppm) δ 137.0, 129.5, 128.9, 127.2, 125.5, 124.4, 122.5, 34.0, 33.4, 22.9, 14.1; MS (DART) calcd for C₂₄H₂₇

314.2, found 314.2 ([M + H]⁺). Anal. Calcd for $C_{24}H_{26}$: C, 91.67; H, 8.33. Found: C, 91.79; H, 8.52.

Synthesis of 1,6-Bis(trimethylsilyl)pyrene (P2e). P2e was synthesized according to Procedure B. Pale yellow solid; yield 61% (1.52 g); mp 224.1−225.8 °C; ¹H NMR (400 MHz, CDCl₃, ppm) δ 8.36 (d, J = 9.1 Hz, 2H), 8.19 (d, J = 7.6 Hz, 2H), 8.16 (d, J = 7.6 Hz, 2H), 8.09 (d, J = 9.1 Hz, 2H), 0.59 (s, 12H); ¹³C NMR (100 MHz, CDCl₃, ppm) δ 135.8, 135.7, 131.9, 131.5, 128.1, 127.1, 124.9, 124.2, 0.6; MS (DART) calcd for $C_{22}H_{26}Si_2$ 346.1573, found 346.1611 ([M]⁺).

General Procedure C: Negishi Cross-Coupling Reaction (P1c and P2c). To a solution of zinc chloride (2.0 equiv) in THF was slowly added dropwise a 1.0 M solution of isopropylmagnesium chloride (2.0 equiv) in THF under an argon atmosphere at 0 °C, and then **1** (1.0 equiv) and [1,1′-bis(diphenylphosphino)ferrocene]-palladium(II) dichloride (5 mol %) were added. The reaction mixture was then heated to reflux for 3 h. After quenching the reaction with water, the organic layer was extracted with chloroform and dried over Na₂SO₄. The solvent was removed in vacuo, and the residue was purified by short-plug column chromatography on silica gel (hexane) and high-performance liquid chromatography. The relevant isomer, e.g., 1-propylpyrene, was isolated by repeated recrystallization in ethanol.

Synthesis of 1-Isopropylpyrene (P1c). P1c was synthesized according to Procedure C, and purified by the recrystallization in ethanol. Colorless crystal; yield 25% (0.33 g); ¹H NMR (400 MHz, CDCl₃, ppm) δ 8.39 (d, J = 9.3 Hz, 1H), 8.18−7.96 (m, 8H), 4.09 (septet, J = 6.4 Hz, 1H), 1.54 (d, J = 6.4 Hz, 6H); MS (DART) calcd for $C_{19}H_{16}$ 244.1, found 244.1 ([M]⁺). Anal. Calcd for $C_{19}H_{16}$: C, 93.40; H, 6.60. Found: C, 93.31; H, 6.48.

Synthesis of 1,6-Diisopropylpyrene (P2c). P2c was synthesized according to Procedure C, using **2** (1.0 equiv), zinc chloride (4.0 equiv), isopropylmagnesium chloride (4.0 equiv), and [1,1′-bis-(diphenylphosphino)ferrocene] (10 mol %). Recrystallization was repeatedly carried out using toluene. Colorless crystal; yield 41% (0.85 g); ¹H NMR (400 MHz, CDCl₃, ppm) δ 8.32 (d, J = 9.5 Hz, 1H), 8.15 (d, J = 8.1 Hz, 1H), 8.06 (d, J = 9.5 Hz, 1H), 7.99 (d, J = 8.1 Hz, 1H), 4.08 (septet, J = 6.8 Hz, 2H), 1.53 (d, J = 6.8 Hz, 3H); MS (DART) calcd for $C_{22}H_{22}$ 286.1, found 286.1 ([M]⁺). Anal. Calcd for $C_{22}H_{22}$: C, 92.26; H, 7.74. Found: C, 92.04; H, 7.75.

General Procedure D: Kumada Cross-Coupling Reaction (P1d and P2d). A mixture of **1** (1.0 equiv), $NiCl_2(H_2O)_{1.5-1.7}$ (10 mol %), and 1,3-dicyclohexylimidazolium tetrafluoroborate (NHC ligand) (10 mol %) was cooled to −10 °C under an argon atmosphere, and then a 1.0 M solution of tert-butylmagnesium chloride (2.0 equiv) in THF was slowly added dropwise; the mixture was stirred for 90 min. The reaction mixture was quenched by addition of ice chips and then poured into a separating funnel containing saturated aqueous NH₄Cl. The organic layer was extracted with chloroform and dried over Na₂SO₄. The solvent was removed in vacuo, and the residue was purified by short-plug column chromatography on silica gel (hexane) and high-performance liquid chromatography. The relevant isomer, e.g., 1-isobutylpyrene, was isolated by repeated recrystallization in ethanol.

Synthesis of 1-tert-Butylpyrene (P1d). P1d was synthesized according to Procedure D and purified by recrystallization in ethanol. Colorless crystal; yield 7% (0.13 g); ¹H NMR (400 MHz, CDCl₃, ppm) δ 8.75 (d, J = 9.5 Hz, 1H), 8.18−7.97 (m, 7H), 1.79 (s, 9H); MS (DART) calcd for $C_{20}H_{18}$ 258.1, found 258.1 ([M]⁺). Anal. Calcd for $C_{20}H_{18}$: C, 92.98; H, 7.02. Found: C, 93.10; H, 7.07.

Synthesis of 1,6-Di(tert-butyl)pyrene (P2d). P2d was synthesized according to Procedure D where **2** (1.0 equiv) as a starting material, $NiCl_2(H_2O)_{1.5-1.7}$ (20 mol %), 1,3-dicyclohexylimidazolium tetrafluoroborate (20 mol %) and tert-butylmagnesium chloride (4.0 equiv) were used. Recrystallization was repeatedly carried out by using toluene. Colorless crystal; yield 5% (0.11 g); ¹H NMR (400 MHz, CDCl₃, ppm) δ 8.68 (d, J = 9.5 Hz, 1H), 1.78 (s, 4H), 8.02 (d, J = 9.5 Hz, 1H), 1.78 (s, 9H); MS (DART) calcd for $C_{24}H_{26}$ 314.2, found 314.2 ([M]⁺). Anal. Calcd for $C_{24}H_{26}$: C, 91.67; H, 8.33. Found: C, 91.84; H, 8.42.

Synthesis of 3-Bromo-1,6-dibutylpyrene (3). To a stirred solution of P2b (0.50 g, 1.6 mmol) and HBr (0.1 mL, 2.0 mmol) in diethyl ether (25 mL) and methanol (10 mL) was added a solution of hydrogen peroxide (0.18 mL, 2.0 mmol) in dichloromethane at 0 °C. This mixture was allowed to gradually warm to room temperature and was then stirred for 12 h. The reaction mixture was poured into a large amount of ice−water and extracted with chloroform. The combined organic layers were washed with NaHCO₃ and brine and dried over MgSO₄. The solvent was removed in vacuo, and the residue was purified by short-plug column chromatography on silica gel (hexane) and high-performance liquid chromatography on polystyrene to give **3** as a colorless solid; **3** was used in the next step without further purification. Yield 80% (0.50 g); ¹H NMR (400 MHz, CDCl₃, ppm) δ 8.44−8.05 (m, 6H), 7.87 (d, J = 7.8 Hz, 1H), 3.33 (t, J = 7.8 Hz, 2H), 3.27 (t, J = 7.8 Hz, 2H), 1.87−1.78 (m, 4H), 1.53−1.47 (m, 4H), 1.00 (t, J = 7.3 Hz, 3H), 0.99 (t, J = 7.4 Hz, 3H); ¹³C NMR (100 MHz, CDCl₃, ppm) δ 137.9, 137.7, 131.0, 129.6, 128.5, 127.9, 127.8, 127.5, 126.8, 125.7, 125.2, 124.9, 124.1, 122.3, 119.4, 34.1, 33.8, 33.4, 33.1, 22.8, 14.0; MS (DART) calcd for $C_{24}H_{26}Br$ 393.1, found 393.1 ([M + H]⁺).

Synthesis of 1,6-Dibromo-3,8-dibutylpyrene (4). To a stirred solution of P2b (0.50 g, 1.6 mmol) in dichloromethane (10 mL) was added dropwise a solution of bromine (0.2 mL, 4.0 mmol) in dichloromethane over 1.5 min at 0 °C. After stirring at room temperature for 30 min, the reaction mixture (an orange suspension) was quenched with methanol. The precipitates were washed with methanol and filtered to give the crude product. Subsequent recrystallization in toluene afforded **4** as a pale yellow solid; **4** was used in the next step without further purification. Yield 67% (2.01 g); ¹H NMR (400 MHz, CDCl₃, ppm) δ 8.45 (d, J = 9.4 Hz, 2H), 8.26 (d, J = 9.4 Hz, 2H), 8.14 (s, 2H), 3.30 (t, J = 7.8 Hz, 4H), 1.83 (tt, J = 7.5 Hz, 7.8 Hz, 4H), 1.54 (tq, J = 7.3 Hz, 7.5 Hz, 4H), 1.00 (t, J = 7.3 Hz, 6H) ppm.

Synthesis of 1,3,6-Tributylpyrene (P3b). P3b was synthesized according to Procedure A. Yellow solid; yield 66% (0.15 g); mp 44.3−46.2 °C; ¹H NMR (400 MHz, CDCl₃, ppm) δ 8.27 (d, J = 9.3 Hz, 1H), 8.23 (d, J = 9.5 Hz, 1H), 8.17 (d, J = 9.3 Hz, 1H), 8.03 (d, J = 7.9 Hz, 1H), 7.97 (d, J = 9.1 Hz, 1H), 7.81 (d, J = 7.9 Hz, 1H), 7.69 (s, 1H), 3.32−3.26 (m, 6H), 1.86−1.78 (m, 6H), 1.55−1.45 (m, 6H), 1.02−0.97 (m, 9H); ¹³C NMR (100 MHz, CDCl₃, ppm) δ 136.6, 136.5, 136.4, 129.8, 128.8, 128.6, 127.4, 127.0, 126.9, 126.3, 126.0, 125.9, 124.2, 123.2, 122.6, 122.2, 34.1, 34.0, 33.5, 33.4, 33.3, 14.1; MS (DART) calcd for $C_{28}H_{35}$ 371.3, found 371.3 ([M + H]⁺). Anal. Calcd for $C_{28}H_{34}$: C, 90.75; H, 9.25. Found: C, 90.50; H, 9.51.

Synthesis of 1,3,6,8-Tetrabutylpyrene (P4b). P4b was synthesized according to Procedure B. Pale yellow needle; yield 68% (0.11 g); mp 97.6−98.8 °C; ¹H NMR (400 MHz, CDCl₃, ppm) δ 8.19 (s, 4H), 7.68 (s, 2H), 3.29 (t, J = 7.8 Hz, 8H), 1.83 (tt, J = 7.5 Hz, 7.8 Hz, 8H), 1.52 (tq, J = 7.4 Hz, 7.5 Hz, 8H), 1.00 (t, J = 7.4 Hz, 12H); ¹³C NMR (100 MHz, CDCl₃, ppm) δ 136.1, 128.7, 127.1, 126.4, 122.2, 34.1, 33.5, 22.9, 14.1; MS (DART) calcd for $C_{32}H_{43}$ 427.3, found 427.3 ([M + H]⁺). Anal. Calcd for $C_{32}H_{42}$: C, 90.08; H, 9.92. Found: C, 89.98; H, 9.52.

ASSOCIATED CONTENT

Ⓢ Supporting Information

Additional experimental methods for pyrenes with alkyl and TMS groups. Results of UV−vis and fluorescence spectra in hexane and methanol solution; dependence of fluorescence properties on solution concentration; square wave voltammograms; DFT/TD-DFT calculations; and ¹NMR and ¹³C NMR spectra. This material is available free of charge via the Internet at http://pubs.acs.org.

AUTHOR INFORMATION

Corresponding Author
*E-mail: konishi.g.aa@m.titech.ac.jp.

Notes

The authors declare no competing financial interest.

■ REFERENCES

(1) Kalyanasundaram, K.; Thomas, J. K. *J. Am. Chem. Soc.* **1977**, *99*, 2039−2044.

(2) Winnik, F. M. *Chem. Rev.* **1977**, *93*, 587−614.

(3) Hashidzume, A.; Zheng, Y. T.; Harada, A. *Beilstein J. Org. Chem.* **2012**, *8*, 1312−1317.

(4) Nagata, Y.; Nishikawa, T.; Suginome, M. *Chem. Commun.* **2012**, *48*, 11193−11195.

(5) Morikawa, M.; Yoshihara, M.; Endo, T.; Kimizuka, N. *Chem.— Eur. J.* **2005**, *11*, 1574−1578.

(6) Karmakar, S.; Anderson, B. A.; Rathje, R. L.; Andersen, S.; Jensen, T. B.; Nielsen, P.; Hrdlicka, P. J. *J. Org. Chem.* **2011**, *76*, 7119−7131.

(7) Sau, S. P.; Hrdlicka, P. J. *J. Org. Chem.* **2012**, *77*, 5−16.

(8) Ingale, S. A.; Pujari, S. S.; Sirivolu, V. R.; Ding, P.; Xiong, H.; Mei, H.; Seela, F. *J. Org. Chem.* **2012**, *77*, 188−199.

(9) Wojciechowski, F.; Lietard, J.; Leumann, C. J. *Org. Lett.* **2012**, *14*, 5176−5179.

(10) Ono, T.; Wang, S. L.; Koo, C. K.; Engstrom, L.; David, S. S.; Kool, E. T. *Angew. Chem., Int. Ed.* **2012**, *51*, 1689−1692.

(11) Kashida, H.; Asanuma, H. *Phys. Chem. Chem. Phys.* **2012**, *14*, 7196−7204.

(12) Fujimoto, K.; Shimizu, H.; Inouye, M. *J. Org. Chem.* **2004**, *69*, 3271−3275.

(13) Takada, T.; Otsuka, Y.; Nakamura, M.; Yamana, K. *Bioorg. Med. Chem.* **2011**, *19*, 6881−6884.

(14) Yamana, K.; Zako, H.; Asazuma, K.; Iwase, R.; Nakano, H.; Murakami, A. *Angew. Chem., Int. Ed.* **2001**, *40*, 1104−1106.

(15) Kashida, H.; Asanuma, H.; Komiyama, M. *Chem. Commun.* **2006**, *0*, 2768−2770.

(16) Niskanen, J.; Wu, C.; Ostrowski, M.; Fuller, G. G.; Tenhu, H.; Hietala, S. *Langmuir* **2012**, *28*, 14792−14798.

(17) Duhamel, J. *Langmuir* **2012**, *28*, 6527−6538.

(18) Nakamura, M.; Fukuda, M.; Takada, T.; Yamana, K. *Org. Biomol. Chem.* **2012**, *10*, 9620−9626.

(19) Ingale, S. A.; Seela, F. *J. Org. Chem.* **2012**, *77*, 9352−9356.

(20) Aoki, I.; Sakaki, T.; Shinkai, S. *J. Chem. Soc., Chem. Commun.* **1992**, 730−732.

(21) Wegner, S. V.; Okesli, A.; Chen, P.; He, C. *J. Am. Chem. Soc.* **2007**, *129*, 3474−3475.

(22) Jang, S.; Thirupathi, P.; Neupane, L. N.; Seong, J.; Lee, H.; Lee, W. I.; Lee, K. H. *Org. Lett.* **2012**, *14*, 4746−4749.

(23) Fernández-Lodeiro, J.; Núñez, C.; de Castro, C. S.; Bértolo, E.; de Melo, J. S. S.; Capelo, J. L.; Lodeiro, C. *Inorg. Chem.* **2013**, *52*, 121−129.

(24) Agudelo-Morales, C. E.; Galian, R. E.; Perez-Prieto, J. *Anal. Chem.* **2012**, *84*, 8083−8087.

(25) Chen, Y. L.; Zhu, B.; Han, Y.; Bo, Z. S. *J. Mater. Chem.* **2012**, *22*, 4927−4931.

(26) Imai, K.; Sasaki, T.; Abe, J.; Nemoto, N. *Polym. Bull.* **2012**, *68*, 1589−1601.

(27) Chan, K. L.; Lim, J. P. F.; Yang, X. H.; Dodabalapur, A.; Jabbour, G. E.; Sellinger, A. *Chem. Commun.* **2012**, *48*, 5106−5108.

(28) Hu, J. Y.; Pu, Y. J.; Nakata, G.; Kawata, S.; Sasabe, H.; Kido, J. *Chem. Commun.* **2012**, *48*, 8434−8436.

(29) Yang, X. H.; Giovenzana, T.; Feild, B.; Jabbour, G. E.; Sellinger, A. *J. Mater. Chem.* **2012**, *22*, 12689−12694.

(30) Thomas, K. R. J.; Kapoor, N.; Bolisetty, M. N. K. P.; Jou, J. H.; Chen, Y. L.; Jou, Y. C. *J. Org. Chem.* **2012**, *77*, 3921−3932.

(31) Diring, S.; Camerel, F.; Donnio, B.; Dintzer, T.; Toffanin, S.; Capelli, R.; Muccini, M.; Ziessel, R. *J. Am. Chem. Soc.* **2009**, *131*, 18177−18185.

(32) Goel, A.; Kumar, V.; Nag, P.; Bajpai, V.; Kumar, B.; Singh, C.; Prakash, S.; Anand, R. S. *J. Org. Chem.* **2011**, *76*, 7474−7481.

(33) Figueira-Duarte, T. M.; Müllen, K. *Chem. Rev.* **2011**, *111*, 7260−7314.

(34) Uchimura, M.; Watanabe, Y.; Araoka, F.; Watanabe, W.; Takezoe, H.; Konishi, G. *Adv. Mater.* **2010**, *22*, 4473−4478.

(35) Watanabe, Y.; Uchimura, M.; Araoka, F.; Konishi, G.; Watanabe, J.; Takezoe, H. *Appl. Phys. Express* **2009**, *2*, 102501.

(36) Takemoto, K.; Karasawa, M.; Kimura, M. *ACS Appl Mater. Interface* **2012**, *4*, 6289−6294.

(37) Lee, O. P.; Yiu, A. T.; Beaujuge, P. M.; Woo, C. H.; Holcombe, T. W.; Millstone, J. E.; Douglas, J. D.; Chen, M. S.; Frechet, J. M. J. *Adv. Mater.* **2011**, *23*, 5359−5363.

(38) Berlman, I. B. *J. Chem. Phys.* **1970**, *74*, 3085−3093.

(39) Nijegorodov, N. I.; Downey, W. S. *J. Phys. Chem.* **1994**, *98*, 5639−5643.

(40) de Halleux, V.; Calbert, J. P.; Brocorens, P.; Cornil, J.; Declercq, J. P.; Brédas, J. L.; Geerts, Y. *Adv. Funct. Mater.* **2004**, *14*, 649−659.

(41) Fujimoto, K.; Shimizu, H.; Furusyo, M.; Akiyama, S.; Ishida, M.; Furukawa, U.; Yokoo, T.; Inouye, M. *Tetrahedron* **2009**, *65*, 9357−9361.

(42) Wojciechowski, F.; Lietard, J.; Leumann, C. J. *Org. Lett.* **2012**, *14*, 5176−5179.

(43) Figueira-Duarte, T. M.; Simon, S. C.; Wagner, M.; Drtezhinin, S. I.; Zachariasse, K. A.; Müllen, K. *Angew. Chem., Int. Ed.* **2008**, *47*, 10175−10178.

(44) Sagara, Y.; Mutai, T.; Yoshikawa, I.; Araki, K. *J. Am. Chem. Soc.* **2007**, *129*, 1520−1521.

(45) Sase, M.; Yamaguchi, S.; Sagara, Y.; Yoshikawa, I.; Mutai, T.; Araki, K. *J. Mater. Chem.* **2011**, *21*, 8347−8354.

(46) Yamaguchi, S.; Yoshikawa, I.; Mutai, T.; Araki, K. *J. Mater. Chem.* **2012**, *22*, 20065−20070.

(47) Shimizu, H.; Fujimoto, K.; Furusyo, M.; Maeda, H.; Nanai, Y.; Mizuno, K.; Inouye, M. *J. Org. Chem.* **2007**, *72*, 1530−1533.

(48) Maeda, H.; Maeda, T.; Mizuno, K.; Fujimoto, K.; Shimizu, H.; Inouye, M. *Chem.—Eur. J.* **2006**, *12*, 824−831.

(49) Sagara, Y.; Kato, T. *Angew. Chem., Int. Ed.* **2008**, *47*, 5175−5178.

(50) Hayer, A.; de Halleux, V.; Köhler, A.; El-Garoughy, A.; Meijer, E. W.; Barberá, J.; Tant, J.; Levin, J.; Lehmann, M.; Gierschner, J.; Cornil, J.; Geerts, Y. H. *J. Phys. Chem. B* **2006**, *110*, 7653−7659.

(51) Venkataramana, G.; Sankararaman, S. *Eur. J. Org. Chem.* **2005**, 4162−4166.

(52) Kim, H. M.; Lee, Y. O.; Lim, C. S.; Kim, J. S.; Cho, B. R. *J. Org. Chem.* **2008**, *73*, 5127−5130.

(53) Wang, G.; Geng, J. L.; Zhang, X. H.; Cai, L. P.; Ding, D.; Li, K.; Wang, L.; Lai, Y. H.; Liu, B. *Polym. Chem.* **2012**, *3*, 2464−2470.

(54) Suenaga, H.; Nakashima, K.; Mizuno, T.; Takeuchi, M.; Hamachi, I.; Shinkai, S. *J. Chem. Soc., Perkin Trans. 1* **1998**, 1263−1267.

(55) Maeda, H.; Inoue, Y.; Ishida, H.; Mizuno, K. *Chem. Lett.* **2001**, *30*, 1224−1225.

(56) Maeda, H.; Ishida, H.; Inoue, Y.; Merpuge, A.; Maeda, T.; Mizuno, K. *Res. Chem. Intermed.* **2009**, *35*, 939−948.

(57) Ara, A. M.; Iimori, T.; Nakabayashi, T.; Maeda, H.; Mizuno, K.; Ohta, N. *J. Phys. Chem. B* **2007**, *111*, 106870−10696.

(58) Asai, K.; Konishi, G.; Sumi, K.; Mizuno, K. *J. Organomet. Chem.* **2011**, *696*, 1236−1243.

(59) Asai, K.; Konishi, G.; Nakajima, Y.; Kawauchi, S.; Ozawa, F.; Mizuno, K. *J. Organomet. Chem.* **2011**, *696*, 1266−1271.

(60) Yamaji, M.; Maeda, H.; Minamida, K.; Maeda, T.; Asai, K.; Konishi, G.; Mizuno, K. *Res. Chem. Inermed.* **2013**, *39*, 321−345.

(61) Shimizu, M.; Tatsumi, H.; Mochida, K.; Hiyama, T. *Chem. Commun.* **2008**, *0*, 2134−2136.

(62) Niko, Y.; Kawauchi, S.; Konishi, G. *Tetrahedron Lett.* **2011**, *52*, 4843−4847.

(63) Niko, Y.; Konishi, G. *Macromolecules* **2012**, *45*, 2327−2337.

(64) Niko, Y.; Hiroshige, Y.; Kawauchi, S.; Konishi, G. *J. Org. Chem.* **2012**, *77*, 3986−3996.

(65) Niko, Y.; Hiroshige, Y.; Kawauchi, S.; Konishi, G. *Tetrahedron* **2012**, *68*, 6177−6185.

(66) Niko, Y.; Konishi, G. *J. Syn. Org. Chem. Jpn* **2012**, *79*, 918−927.

(67) Wang, G.; Geng, J. L.; Zhang, X. H.; Cai, L. P.; Ding, D.; Li, K.; Wang, L.; Lai, Y. H.; Liu, B. *Polym. Chem.* **2012**, *3*, 2464−2470.

(68) Rihn, S.; Retailleau, P.; De Nicola, A.; Ulrich, G.; Ziessel, R. *J. Org. Chem.* **2012**, *77*, 8851−8863.

(69) Shellaiah, M.; Wu, Y. H.; Singh, A.; Ramakrishnam, M. V. R.; Lin, H.-C. *J. Mater. Chem. A* **2013**, *1*, 1310−1318.

(70) Bag, S. S.; Kundu, R. *J. Org. Chem.* **2011**, *76*, 3348−3356.

(71) Wrona-Piotrowicz, A.; Plażuk, D.; Domagała, S.; Zakrzewski, J. *ARKIVOC* **2012**, *6*, 412−420.

(72) Sumi, K.; Konishi, G. *Molecules* **2010**, *15*, 7582−7592.

(73) Chen, W. H.; Liaw, D. J.; Wang, K. L.; Lee, K. R.; Lai, J. Y. *Polymer* **2009**, *50*, 5211−5219.

(74) Liaw, D. J.; Wang, K. L.; Chang, F. C. *Macromolecules* **2007**, *40*, 3568−3574.

(75) Lian, W. R.; Wu, H. Y.; Wang, K. L.; Liaw, D. J.; Lee, K. R.; Lai, J. Y. *J. Polym. Sci., Part A: Polym. Chem.* **2011**, *49*, 3673−3680.

(76) Lian, W. R.; Ho, C.; Huang, Y. C.; Liao, Y. A.; Wang, K. L.; Liaw, D. J.; Lee, K. R.; Lai, J. Y. *J. Polym. Sci., Part A: Polym. Chem.* **2011**, *49*, 5350−5357.

(77) Lian, W. R.; Liao, Y. A.; Li, L. J.; Su, C. Y.; Liaw, D. J.; Lee, K. R.; Lai, J. Y. *Macromolecules* **2011**, *44*, 9550−9555.

(78) Li, S.; Han, J.; Gao, C. *Polym. Chem.* **2013**, *4*, 1774−1787.

(79) Yang, Y. X.; Mannion, M. R.; Dawe, L. N.; Kraml, C. M.; Pascal, R. A.; Bodwell, G. J. *J. Org. Chem.* **2012**, *77*, 57−67.

(80) Inouye, M.; Fujimoto, K.; Furusyo, M.; Nakazumi, H. *J. Am. Chem. Soc.* **1999**, *121*, 1452−1458.

(81) Schazmann, B.; Alhashimy, N.; Diamond, D. *J. Am. Chem. Soc.* **2006**, *128*, 8607−8614.

(82) Kokado, K.; Iwamura, T.; Chujo, Y. *Polym. J.* **2008**, *40*, 402−408.

(83) Kajiwara, Y.; Nagai, A.; Chujo, Y. *Chem. Lett.* **2010**, *39*, 480−481.

(84) Eaborn, C.; Lasocki, Z.; Sperry, J. A. *J. Organomet. Chem.* **1972**, *35*, 245−252.

(85) Reynders, P.; Kuhnle, W.; Zachariasse, K. A. *J. Am. Chem. Soc.* **1990**, *112*, 3929−3939.

(86) Ionkin, A. S.; Marshall, W. J.; Fish, B. M. *Organometallics* **2006**, *25*, 1461−1471.

(87) Sato, M.; Tanaka, S.; Kaeriyama, K. *J. Chem. Soc., Chem. Commun.* **1986**, *11*, 873−874.

(88) Clar, E.; McAndrew, B. A.; Sanigök, Ü. *Tetrahedron* **1970**, *29*, 2099−2105.

(89) Berg, A.; Lam, J.; Hansen, P. E. *Acta Chem. Scand.* **1986**, *40b*, 665−677.

(90) Hansen, P. E.; Berg, A.; Lund, H. *Acta Chem. Scand.* **1976**, *30b*, 267−270.

(91) Banerjee, M.; Vyas, V. S.; Lindeman, S. V.; Rathore, R. *Chem. Commun.* **2008**, *0*, 1889−1891.

(92) Li, J.; Takaishi, S.; Fujinuma, N.; Endo, K.; Yamashita, M.; Matsuzaki, H.; Okamoto, H.; Sawabe, K.; Takenobu, T.; Iwasa, Y. *J. Mater. Chem.* **2011**, *21*, 17662−17666.

(93) Fukuda, M.; Sawada, K.; Yoshino, K. *Jpn. J. Appl. Phys.* **1989**, *28*, 1433−1435.

(94) Sato, M.; Tanaka, S.; Kaeriyama, K. *J. Chem. Soc., Chem. Commun.* **1986**, *11*, 873−874.

(95) Nijegorodov, N.; Vasilenko, V.; Monowe, P.; Masale, M. *Spectrochim. Acta A* **2009**, *74*, 188−194.

(96) Sato, A. H.; Maeda, M.; Mihara, S.; Iwasawa, T. *Tetrahedron Lett.* **2011**, *52*, 6284−6287.

(97) Joshi-Pangu, A.; Wang, C. Y.; Biscoe, M. R. *J. Am. Chem. Soc.* **2011**, *133*, 8478−8481.

(98) Minabe, M.; Takeshige, S.; Soeda, Y.; Kimura, T.; Tsubota, M. *Bull. Chem. Soc. Jpn.* **1994**, *67*, 172−179.

(99) Kyusin, S.; Ikarugi, M.; Goto, M.; Hiratsuka, H.; Matsumoto, H. *Organometallics* **1996**, *15*, 1067−1070.

(100) Yamaguchi, S.; Tamao, K. *Bull. Soc. Chem. Jpn.* **1996**, *69*, 2327−2334.

(101) Tamao, K.; Uchida, M.; Izumizawa, T.; Furukawa, K.; Yamaguchi, S. *J. Am. Chem. Soc.* **1996**, *118*, 11974−11975.

(102) Uchida, M.; Izumizawa, T.; Nakano, T.; Yamaguchi, S.; Tamao, K.; Furukawa, K. *Chem. Mater.* **2001**, *13*, 2680−2683.

(103) Yamaguchi, S.; Endo, T.; Uchida, M.; Izumizawa, T.; Furukawa, K.; Tamao, K. *Chem.—Eur. J.* **2000**, *6*, 1683−1692.

(104) Negishi, E.; King, A. O.; Okukado, N. *J. Org. Chem.* **1977**, *42*, 1821−1823.

(105) Tamao, K.; Sumitani, K.; Kumada, M. *J. Am. Chem. Soc.* **1972**, *94*, 4374−4376.

(106) Tamao, K.; Sumitani, K.; Kiso, Y.; Zembayashi, M.; Fujioka, A.; Kodama, S.; Nakajima, I.; Minato, A.; Kumada, M. *Bull. Chem. Soc. Jpn.* **1976**, *49*, 1958−1969.

(107) Hayashi, T.; Konishi, M.; Kobori, Y.; Kumada, M.; Higuchi, T.; Hirotsu, K. *J. Am. Chem. Soc.* **1984**, *106*, 158−163.

(108) Chai, J.-D.; Head-Gordon, M. *Phys. Chem. Chem. Phys.* **2008**, *10*, 6615−6620.

(109) Ditchfield, R.; Hehre, W. J.; Pople, J. A. *J. Chem. Phys.* **1971**, *54*, 724−728.

(110) Hehre, W. J.; Ditchfield, R.; Pople, J. A. *J. Chem. Phys.* **1972**, *56*, 2257−2261.

(111) Hariharan, P. C.; Pople, J. A. *Theor. Chem. Acc.* **1973**, *28*, 213−222.

(112) Hariharan, P. C.; Pople, J. A. *Mol. Phys.* **1974**, *27*, 209−214.

(113) Mardirossian, N.; Parkhill, J. A.; Head-Gordon, M. *Phys. Chem. Chem. Phys.* **2011**, *13*, 19325−19337.

(114) Jacquemin, D.; Perpète, E. A.; Ciofini, I.; Adamo, C. *Theor. Chem. Acc.* **2011**, *128*, 127−136.

(115) Turro, N. J.; Ramamurthyl, V.; Scaiano, J. C. *Modern Molecular Photochemistry of Organic Molecules*; University Science Books: Sausalito, CA, 2010. (a) Ham effect: p 912; (b) Internal conversion rate constant of polycyclic aromatic hydrocarbons: pp 300−305; (c) Energy gap Law: p 310; and (d) Loose-bolt effect: pp 288−294.

(116) Eakins, G. L.; Alford, J. S.; Tiegs, B. J.; Breyfogl, B. E.; Stearn, C. J. *J. Phys. Org. Chem.* **2011**, *24*, 1119−1128.

(117) Figueira-Duarte, T. M.; Rosso, P. G. D.; Trattnig, R.; Sax, S.; List, E. J. W.; Müllen, K. *Adv. Mater.* **2010**, *22*, 990−993.

(118) Oh, H. Y.; Lee, C.; Lee, S. *Org. Electron.* **2009**, *10*, 163−169.

(119) Hong, Y.; Lam, J. W. Y.; Tang, B. Z. *Chem. Soc. Rev.* **2011**, *40*, 5361−5388.

(120) Katoh, R.; Suzuki, K.; Furube, A.; Kotani, M.; Tokumaru, K. *J. Phys. Chem. C* **2009**, *113*, 2961−2965.